

Alkali Metal- and Acid-Catalyzed Interconversion of Goniiodomin A with Congeners B and C

Constance M. Harris, Bernd Krock, Urban Tillmann, Craig J. Tainter, Donald F. Stec, Aaron J. C. Andersen, Thomas O. Larsen, Kimberly S. Reece, and Thomas M. Harris*

Cite This: *J. Nat. Prod.* 2021, 84, 2554–2567

Read Online

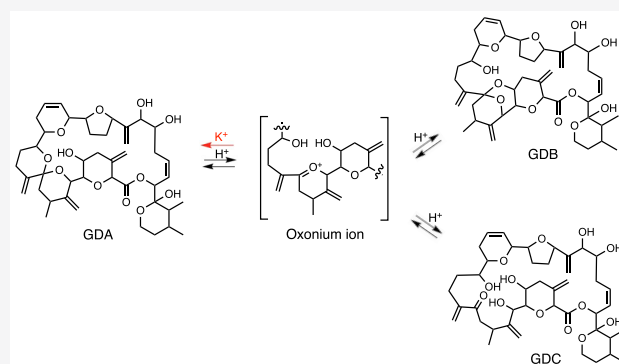
ACCESS |

Metrics & More

Article Recommendations

Supporting Information

ABSTRACT: Goniiodomin A (GDA, **1**) is a phycotoxin produced by at least four species of *Alexandrium* dinoflagellates that are found globally in brackish estuaries and lagoons. It is a linear polyketide with six oxygen heterocyclic rings that is cyclized into a macrocyclic structure via lactone formation. Two of the oxygen heterocycles in **1** comprise a spiro-bis-pyran, whereas goniiodomin B (GDB) contains a 2,7-dioxabicyclo[3.3.1]nonane ring system fused to a pyran. When H₂O is present, **1** undergoes facile conversion to isomer GDB and to an α,β -unsaturated ketone, goniiodomin C (GDC, **7**). GDB and GDC can be formed from GDA by cleavage of the spiro-bis-pyran ring system. GDA, but not GDB or GDC, forms a crown ether-type complex with K⁺. Equilibration of GDA with GDB and GDC is observed in the presence of H⁺ and of Na⁺, but the equilibrated mixtures revert to GDA upon addition of K⁺. Structural differences have been found between the K⁺ and Na⁺ complexes. The association of GDA with K⁺ is strong, while that with Na⁺ is weak. The K⁺ complex has a compact, well-defined structure, whereas Na⁺ complexes are an ill-defined mixture of species. Analyses of in vitro *A. monilatum* and *A. hiraoui* cultures indicate that only GDA is present in the cells; GDB and GDC appear to be postharvest transformation products.



Goniiodomin A (GDA, **1**, Figure 1), a polyketide phycotoxin produced by dinoflagellates in the *Alexandrium* genus, was isolated in 1968 as the product of a Puerto Rican algal bloom of an unidentified *Alexandrium* species.^{1,2} It was rediscovered 20 years later by Murakami et al. as a metabolite of *Alexandrium hiraoui* (initially named *Goniodoma pseudogonyaulax*).³ Murakami's group established the structure, and after yet another two decades Takeda et al. established the absolute configuration.⁴ GDA contains six oxygen heterocycles. Takeda's configurational assignments rested heavily on the assumption that GDA was conformationally constrained by five of the heterocyclics being imbedded in the macrolide ring. Speculation that errors might be present in Takeda's configurational assignments⁵ has led to major synthetic efforts directed toward configurationally defined total syntheses.^{6–11} Using X-ray crystallography, we recently confirmed the Takeda structure including the absolute configuration.¹² Takeda was able to deduce the conformation of **1** through the use of NOESY spectra and vicinal H–H coupling constants.¹³ The broad features of Takeda's conformation have also been confirmed by the crystallographic structure.¹²

During the course of Takeda's studies of GDA, he isolated a congener, termed goniiodomin B (GDB), which was found in quantities comparable to those of GDA in a sample of GDA he had received from Murakami.¹³ The two compounds are isobaric (MW 768) with empirical formulas of C₄₃H₆₀O₁₂.

They have similar UV spectra with only end absorption at 200 nm, i.e., no accessible chromophore. GDB is more polar than GDA and elutes significantly faster from C18 chromatography columns. Takeda observed partial conversion of GDA to GDB during HPLC purification. He proposed structure **2** for GDB (see Figure 1) on the basis of NMR studies, where differences between the spectra of GDA and GDB were minimal other than in rings A–C. One might have suspected the structural difference between GDA and GDB lay in the configuration of the C-11 ketal, comparable to observations with pectenotoxin,¹⁴ but after protection of the C-26–C-27 vicinal diols as an acetonide, treatment of GDB with acetic anhydride/pyridine yielded an acetyl derivative on the 15-OH. The less shielded chemical shift of H-15 of acetylated GDB relative to the parent toxin led Takeda to conclude that the oxygen linkage between C-11 and C-15 had been replaced by a linkage between C-5 and C-11, creating a 2,7-dioxabicyclo[3.3.1]nonane ring system in GDB. The configurations of substituents on the

Received: June 20, 2021

Published: September 14, 2021



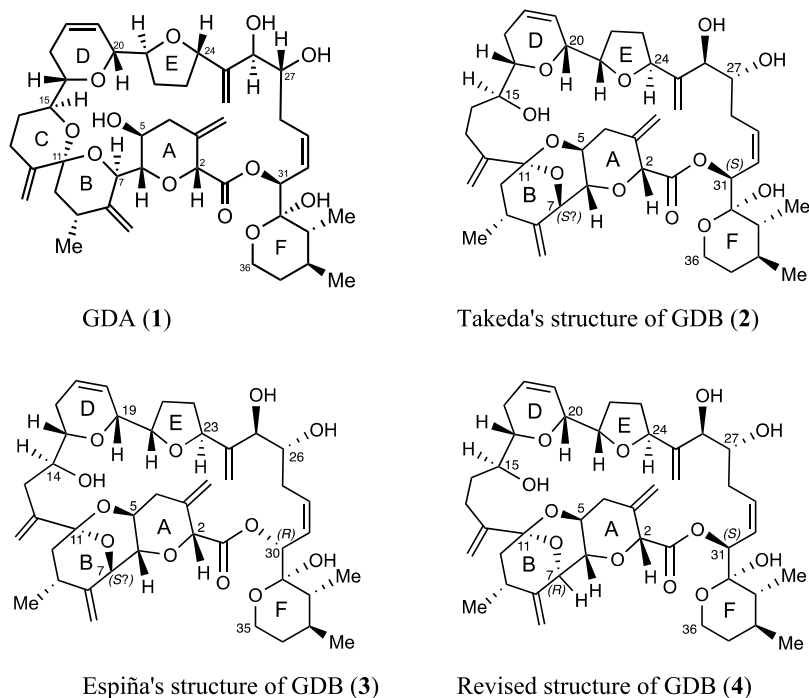


Figure 1. Structures of goniodomins A and B.

dioxabicyclononane ring of GDB were deduced from NOEs. Key NOEs are depicted in Figure 2. The spectroscopic and chemical studies by which Takeda deduced the structure of GDB are described in detail in his Ph.D. dissertation.¹³

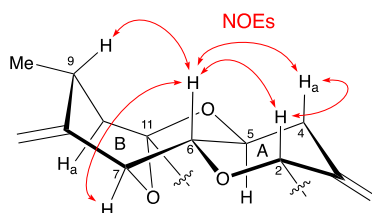


Figure 2. Key NOEs observed by Takeda for GDB. Adapted from ref 13.

We became interested in the interconversion of GDA with its congeners after observing gradual conversion of GDA to GDB when GDA was stored in solution. In the present paper, the structure of GDB is revisited and a revision of Takeda's structure is proposed. An additional congener, goniodomin C (GDC, 7), has been identified. The mechanism of interconversion of GDA with GDB and GDC has been examined, leading to the discovery of a unique cation effect that controls the equilibrium point. Namely, introduction of a potassium ion into equilibrated mixtures causes GDB and GDC to revert to GDA. Facile interconversion of these three species complicates establishing whether all three are truly natural products, but the evidence is compelling for GDA.

RESULTS AND DISCUSSION

Structure Revision of Goniodomin B. An investigation of the structure of GDB was carried out prior to gaining access to Takeda's Ph.D. dissertation.¹³ Electrospray mass spectrometry conducted in MeOH gave an intense signal, m/z 791.3962, for the adduct formed by adventitious Na^+ along

with weaker signals for NH_4^+ and K^+ adducts; the H^+ adduct was not observed. A mass spectrum acquired after addition of the chloride salts of Li, Na, K, Rb, and Cs showed strong preference for addition of Li^+ in contrast to the situation with GDA, where strong preference for K^+ , Rb^+ , and Cs^+ was observed.¹² The exact masses of adduct peaks of GDB were consistent with an empirical formula of $\text{C}_{43}\text{H}_{60}\text{O}_{12}$, which confirmed that proposed by Takeda.

NMR data for GDB obtained in the present study along with those for GDA and GDB in Takeda's dissertation¹³ are presented in Table 1. The NMR spectrum of GDB prepared in the present study is essentially identical to Takeda's. In the present study, peak assignments for GDB were made based on two- and three-bond ^1H – ^1H connectivities obtained from a COSY spectrum, one-bond ^1H – ^{13}C connectivities obtained from an HSQC spectrum, and two- and three-bond ^1H – ^{13}C connectivities obtained from an HMBC spectrum. These results confirm Takeda's assignments. Relative configurations in the region of C-11 were established by NOEs observed between H-6 and H-2, H-4, H-7, and H-9, all being on one face of the eight-membered ring. These NOEs are the same as those reported by Takeda.

Espiña et al., collaborating with Takeda and Sasaki, reported toxicity studies of GDB.¹⁵ In their paper the structure of GDB was depicted as 3, which contained multiple errors. A very serious one involved deletion of a methylene group between C-11 and C-14, leading to an apparent empirical formula of $\text{C}_{42}\text{H}_{58}\text{O}_{12}$. This structural problem was compounded when Krock et al., assuming the correctness of Espiña's GDB structure, quite remarkably found a congener having a molecular weight of 754 being formed by *A. pseudogonyaulax* and wrongly concluded it was GDB.^{16,17} In fact, this truncated analogue of GDA involves deletion of a methyl group from ring F, most likely from C-34.¹⁸

A second error involved the configuration at C-31. This error may be minor, although it would have significant

Table 1. NMR Spectra of GDA, GDB, and GDC

| | goniodomin A (1) ^a | | goniodomin B ^b | | goniodomin B (4) ^c | | goniodomin C (7) ^a | |
|--------|-------------------------------|---------------------------|---------------------------|------------------------------|-------------------------------|----------------------------|-------------------------------|----------------------------|
| | δ_c | δ_H (J in Hz) | δ_c | δ_H (J in Hz) | δ_c | δ_H (J in Hz) | δ_c | δ_H (J in Hz) |
| 1 | 168.6 | N.P. | 168.6 | N.P. | 168.7 | N.P. | 169.4 | N.P. |
| 2 | 76.4 | 4.21, brs | 78.9 | 4.21, s | 78.5 | 4.16, s | 78.4 | 4.44, s |
| 3 | 140.7 | N.P. | 140.4 | N.P. | 140.5 | N.P. | 140.5 | N.P. |
| 3=CHa | 112.0 | 4.76, s | 114.2 | 4.76, s | 113.9 | 4.74, s | 111.7 | 4.80, s |
| 3=CHb | 112.0 | 4.99, s | 114.2 | 4.96, s | 113.9 | 4.96, s | 111.7 | 5.01, s |
| 4a | 41.4 | 2.29, dd (13.2, 12.0) | 39.4 | 2.20, m | 39.2 | 2.18, m | 40.7 | 2.23, dd (11.2, 11.2) |
| 4b | 41.4 | 2.78, dd (13.2, 5.4) | 39.4 | 2.61, dd (12.0, 4.2) | 39.2 | 2.59, dd (12.5, 4.4) | 40.7 | 2.67, dd (13.6, 5.2) |
| 5 | 70.9 | 4.10, m | 67.9 | 3.83, m | 67.6 | 3.83, m | 69.0 | 3.84, m |
| 5-OH | N.P. | 4.31, s | N.P. | N.O. | N.P. | N.O. | N.P. | N.O. |
| 6 | 80.8 | 3.62, dd (8.4, 8.4) | 82.6 | 3.24, dd (9.6, 2.4) | 82.3 | 3.23, dd (9.2, 2.6) | 82.9 | 3.48, dd (8.6, 5.7) |
| 7 | 73.6 | 5.09, d (8.4) | 79.3 | 4.57, d (2.4) | 79.2 | 4.57, d (2.4) | 76.3 | 4.52, d (5.6) |
| 8 | 149.2 | N.P. | 148.5 | N.P. | 148.7 | N.P. | 154.1 | N.P. |
| 8=CHa | 108.0 | 4.92, s | 108.9 | 4.71, s | 108.6 | 4.70, s | 111.6 | 4.87, s |
| 8=CHb | 108.0 | 5.15, s | 108.9 | 4.91, s | 108.6 | 4.88, s | 111.6 | 5.38, s |
| 9 | 34.5 | 2.53, m | 28.2 | 2.77, m | 28.0 | 2.75, m | 31.0 | 2.98, m |
| 9-Me | 20.8 | 1.38, d (7.2) | 17.1 | 0.92, d (6.6) | 17.0 | 0.90, d (6.6) | 22.0 | 1.08, d (6.9) |
| 10a | 44.3 | 1.71, dd (13.8, 6.6) | 43.6 | 1.47, dd (12.6, 12.6) | 43.4 | 1.47, dd (12.7, 12.7) | 32.7 | 2.31, obscured |
| 10b | 44.3 | 2.11, dd (13.8, 6.0) | 43.6 | 1.78, dd (12.6, 5.4) | 43.4 | 1.77, dd (12.7, 12.7) | 32.7 | 2.96, obscured |
| 11 | 100.4 | N.P. | 101.6 | N.P. | 101.6 | N.P. | 203.4 | N.P. |
| 12 | 150.4 | N.P. | 151.4 | N.P. | 151.4 | N.P. | 150.2 | N.P. |
| 12=CHa | 110.4 | 4.68, s | 112.9 | 4.93, s | 112.6 | 4.93, s | 123.5 | 5.35, s |
| 12=CHb | 110.4 | 4.92, s | 112.9 | 5.36, s | 112.6 | 5.37, s | 123.5 | 5.55, s |
| 13a | 27.7 | 1.97, m | 26.8 | 2.30, m | 26.7 | 2.32, m | 28.0 | 2.31, obscured |
| 13b | 27.7 | 1.99, m | 26.8 | 2.48, ddd (14.4, 8.4, 5.4) | 26.7 | 2.49, ddd (14.5, 8.5, 5.7) | 28.0 | 2.62, dd (14.2, 7.8) |
| 14a | 25.5 | 1.22, m | 34.6 | 1.90, m | 34.5 | 1.91, m | 33.1 | 1.42, m |
| 14b | 25.5 | 1.38, m | 34.6 | 2.03, m | 34.5 | 2.03, m | 33.1 | 1.56, m |
| 15 | 76.4 | 3.69, ddd (9.6, 9.6, 9.6) | 72.6 | 3.53, dd (6.0, 5.4, 3.0) | 72.5 | 3.52, dd (6.1, 6.1, 2.8) | 72.6 | 3.24, m |
| 15-OH | N.P. | N.P. | N.P. | N.O. | N.P. | N.O. | N.P. | N.O. |
| 16 | 77.0 | 3.80, ddd (9.6, 9.6, 9.6) | 75.2 | 3.47, ddd (10.7, 3.0, 3.0) | 74.9 | 3.46, ddd (10.7, 3.0, 3.0) | 76.3 | 3.28, ddd (10.5, 3.9, 3.9) |
| 17a | 27.7 | 1.50, m | 27.3 | 1.61, m | 27.3 | 1.59, m | 26.7 | 1.50, m |
| 17b | 27.7 | 1.55, m | 27.3 | 2.39, m | 27.3 | 2.39, m | 26.7 | 2.07, m |
| 18 | 123.7 | 5.63, brdd (10.8, 5.4) | 125.5 | 5.70, m | 125.1 | 5.70, m | 125.3 | 5.64, m |
| 19 | 129.7 | 6.23, brd (10.8) | 128.4 | 5.94, brd (10.2) | 128.2 | 5.93, brd (10.3) | 127.2 | 5.65, m |
| 20 | 76.8 | 4.37, brd (9.0) | 77.9 | 4.00, brd (4.8) | 77.6 | 4.01, brs | 77.4 | 4.07, brs |
| 21 | 82.0 | 4.01, ddd (9.0, 8.4, 7.2) | 81.7 | 3.85, m | 81.4 | 3.85, m | 73.2 | 3.88, m |
| 22a | 30.7 | 2.25, m | 29.5 | 2.01, m | 29.3 | 2.00, m | 27.6 | 1.86, m |
| 22b | 30.7 | 2.25, m | 29.5 | 2.05, m | 29.3 | 2.05, m | 27.6 | 1.86, m |
| 23a | 31.8 | 1.57, m | 31.5 | 1.73, brddd (11.4, 8.4, 7.7) | 31.4 | 1.73, m | 31.1 | 1.77, m |
| 23b | 31.8 | 2.14, m | 31.5 | 2.33, m | 31.4 | 2.33, m | 31.1 | 2.07, m |
| 24 | 79.8 | 5.19, m | 79.9 | 4.85, brdd (7.2, 6.6) | 79.7 | 4.85, brdd (8.4, 6.3) | 80.5 | 4.68, brdd (8.7, 5.2) |
| 25 | 147.9 | N.P. | 147.9 | N.P. | 148.0 | N.P. | 148.0 | N.P. |
| 25=CHa | 113.2 | 5.04, s | 113.8 | 5.13, s | 113.4 | 5.13, s | 113.0 | 5.23, s |

Table 1. continued

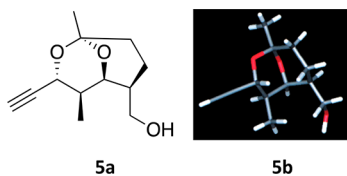
| | goniodomin A (1) ^a | | goniodomin B ^b | | goniodomin B (4) ^c | | goniodomin C (7) ^a | |
|--------|-------------------------------|------------------------------------|---------------------------|-----------------------------|-------------------------------|-----------------------------|-------------------------------|-----------------------------|
| | δ_C | δ_H (J in Hz) | δ_C | δ_H (J in Hz) | δ_C | δ_H (J in Hz) | δ_C | δ_H (J in Hz) |
| 25=CHb | 113.2 | 5.06, s | 113.8 | 5.22, s | 113.4 | 5.20, s | 113.0 | 5.27, s |
| 26 | 81.4 | 4.05, m | 80.2 | 4.07, brd (6.0) | 80.0 | 4.08, d (6.5) | 77.2 | 4.17, brd (4.5) |
| 26-OH | N.P. | N.O. | N.P. | N.O. | N.P. | N.O. | N.P. | N.O. |
| 27 | 73.3 | 3.91, m | 72.9 | 3.83, m | 72.7 | 3.85, m | 80.8 | 3.90, obscured |
| 27-OH | N.P. | 2.89, d (2.4) | N.P. | N.O. | N.P. | N.O. | N.P. | N.O. |
| 28a | 32.7 | 2.10, m | 32.6 | 2.18, m | 32.6 | 2.19, m | 45.8 | 2.35, m |
| 28b | 32.7 | 2.96, dd (13.2, 12.0) | 32.6 | 3.09, dd (12.6, 12.6) | 32.6 | 3.11, dd (12.7, 12.7) | 45.8 | 2.91, dd (16.7, 9.7) |
| 29 | 136.2 | 6.42, ddd (12.0, 11.4, 3.6) | 136.1 | 6.35, ddd (12.6, 10.8, 3.0) | 135.8 | 6.38, ddd (11.5, 11.5, 3.1) | 134.7 | 6.17, ddd (10.8, 10.8, 4.1) |
| 30 | 123.7 | 5.84, dd (11.4, 10.2) | 124.1 | 5.87, dd (10.8, 10.8) | 123.8 | 5.88, dd (10.8, 10.8) | 124.5 | 5.87, d (10.6) |
| 31 | 73.9 | 5.93, d (10.2) | 73.7 | 6.04, d (10.8) | 123.8 | 6.05, d (10.4) | 74.1 | 6.01, d (9.8) |
| 32 | 97.7 | N.P. | 97.8 | N.P. | 98.1 | N.P. | 97.7 | N.P. |
| 32-OH | N.P. | 2.35, d (1.8) | N.P. | N.O. | N.P. | N.O. | N.P. | N.O. |
| 33 | 41.5 | 1.30, m | 41.7 | 1.29, m | 41.5 | 1.30, m | 41.3 | 1.32, m |
| 33-Me | 13.0 | 0.97, d (6.6) | 12.9 | 0.99, d (7.2) | 12.8 | 0.99, d (6.7) | 13.3 | 1.03, d (6.6) |
| 34 | 31.1 | 1.67, m | 31 | 1.67, m | 30.8 | 1.68, m | 31.0 | 1.68, m |
| 34-Me | 20.1 | 0.74, d (6.6) | 20.1 | 0.75, d (6.6) | 19.9 | 0.74, d (6.5) | 20.0 | 0.74, d (6.6) |
| 35a | 34.6 | 1.13, dddd (13.2, 12.6, 12.0, 4.8) | 34.6 | 1.16, m | 34.5 | 1.13, m | 34.6 | 1.15, m |
| 35b | 34.6 | 1.16, m | 34.6 | 1.19, m | 34.5 | 1.16, m | 34.6 | 1.15, m |
| 36a | 60.5 | 3.54, brdd (10.8, 4.2) | 60.5 | 3.56, brdd (10.2, 3.6) | 60.3 | 3.56, dd (10.4, 4.2) | 60.3 | 3.54, brd (10.8) |
| 36b | 60.5 | 3.88, brdd (10.8, 10.8) | 60.5 | 3.91, ddd (13.2, 10.2, 3.0) | 60.3 | 3.89, ddd (11.7, 11.7, 2.8) | 60.3 | 3.88, obscured |

^aReference 4. ^bReference 13. ^cThis work. N.P. = not present; N.O. not observed. Chemical shifts and coupling constants for GDA, GDB, and GDC were measured in benzene-*d*₆. GDC chemical shifts for CH₃, CH₂, and CH signals were determined by HSQC; signals for nonprotonated carbons were determined by HMBC.

consequences for the conformation of the lactone ring and could impact the chemistry and biology of GDB. A third error in Espina's structure of GDB involved the configuration of the oxygen bridge of the dioxabicyclo[3.3.1]nonane ring system, where the oxygen bridge extends from C-7 on the top face of the nine-membered ring to the bottom face of C-11. This error was ported over from the structure 2 of GDB in Takeda's dissertation, which also showed a *trans* oxygen bridge. Molecular mechanics calculations of the energies of *cis* and *trans* 2,9-dioxabicyclo[3.3.1]nonanes indicate the *cis* form would be favored over the *trans* by >38 kcal/mol, meaning the highly strained *trans* bridge would not be present in detectable amounts.

A related error involves the absolute configuration at C-7, which, as pictured in structures 2 and 3, is undefined due to the unidentified location of the inferred proton on C-11. If placed to the right of C-7, the configuration of C-7 becomes *S*; if placed to the left, C-7 becomes *R*. The more reasonable location would be to the right, creating an *S* configuration. Nevertheless, Takeda's structural studies of GDA and our X-ray-derived crystal structure firmly establish the configuration of C-11 in GDA as *R*. Therefore, the configuration of C-11 in GDB is *R* also.

A survey of dioxabicyclo[3.3.1]nonanes reported in SciFinder supports this conclusion. In cases where configuration has been addressed, for example, azaspiracid, a *cis* configuration has been assigned.¹⁹ A few SciFinder abstracts show *trans* configurations, but they are not supported by experimental evidence in the underlying publications. In the abstract for a paper by Nicolaou et al. on the total synthesis of sanglifehrin, SciFinder shows 5a (CA#2341222-54-4) with a *trans* bridge for the 3-ethynyl-1,4-dimethyl-2,9-dioxabicyclo[3.3.1]nonane-6-methanol precursor, but the structure 5b obtained by X-ray crystallography definitively established a *cis* bridge.²⁰



Sasaki's group, working with synthetic compounds that model rings A, B, and C of GDA, observed acid-catalyzed equilibration between models of GDA and GDB.^{11,21} The species that models GDB was shown as 6a with a *trans* bridge, but the configuration was indicated as being identical to that of model compound 6b, for which the three-dimensional structure has a *cis* bridge (Figure 3). They established by NOEs on model compound 6b that the oxygen bridge between C-7 and C-11 is on the back face of the ring and is a *cis* linkage²¹ not the *trans* linkage (2) appearing in Takeda's dissertation.¹³ In that case, SciFinder corrected the error (CA#1268455-91-9), showing the *cis* bridge. The linear depiction of the bonds of C-7, with C-6 and C-8 in 2 and 6a in Figures 1 and 3, respectively, leaves the configuration of C-7 unassigned. Ambiguity concerning the configuration can be removed from the structure by adding the proton at C-7, i.e., the revised structure 4.

Goniodomin C (GDC; 7). GDC was discovered during the present studies of the conversion of GDA to GDB. When the reaction was monitored by HPLC, a third peak with a much shorter retention time than GDA and GDB was observed. Furthermore, the ratio of GDA:GDB:GDC reached a plateau,

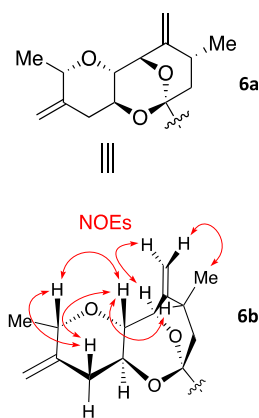
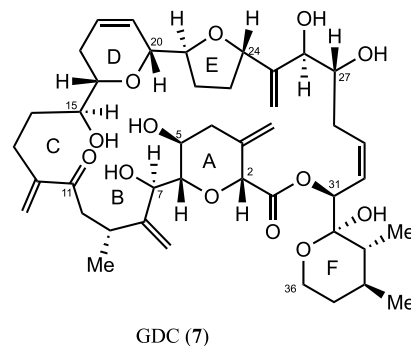


Figure 3. *Cis* linkage of the oxygen bridge of model compound 6b established by NOEs shown as double-headed red arrows.^{11,12}

indicating that equilibration was occurring. HPLC showed 7 is formed in substantial quantities in 1:1 aqueous MeOH. Preparative HPLC was used to produce sufficient amounts of 7 and the other two for chemical characterization and to create analytical standards.



ESI-MS of the Na⁺ adduct of GDC revealed the molecular weight to be 18 Da higher than those of GDA and GDB, indicating addition of one molecule of H₂O. NMR data of 7, acquired using two-dimensional methods, are presented in Table 1. Assigned 2D spectra are available in the Supporting Information. The ¹³C NMR signal observed for C-11 at 203.4 ppm in the HMBC spectrum is consistent with 7 being a ketone. By comparison, the C-11 signals for GDA and GDB are at 100.4 and 101.6 ppm, respectively, which are appropriate for ketals. The 203.4 ppm peak showed strong HMBC cross-peaks to H-10b, 12=CHa, and 12=CHb, firmly identifying C-11 as the carbonyl group of an α,β -unsaturated keto group. HMBC cross-peaks from C-11 to H-10a, H-13a, and H-13b were also observed. Cross-peaks from C-11 to H-7 and H-15 were not observed, which is consistent with the ketal linkages of rings B and C having been disrupted. The 12=CHa and 12=CHb protons of GDC were shifted to higher chemical shifts relative to their counterparts in GDA and GDB and similarly 12=C, supporting conjugation of the double bond with the carbonyl group. The UV spectrum showed a λ_{\max} of 222 nm, which is consistent with GDC containing an α,β -unsaturated keto group. These spectroscopic data establish structure 7 for GDC.

The observed chemical and spectroscopic characteristics of 7 are consistent with previous observations with model compounds that were studied during development of synthetic approaches to GDA.^{8,21–23} Takeda reported that GDA and

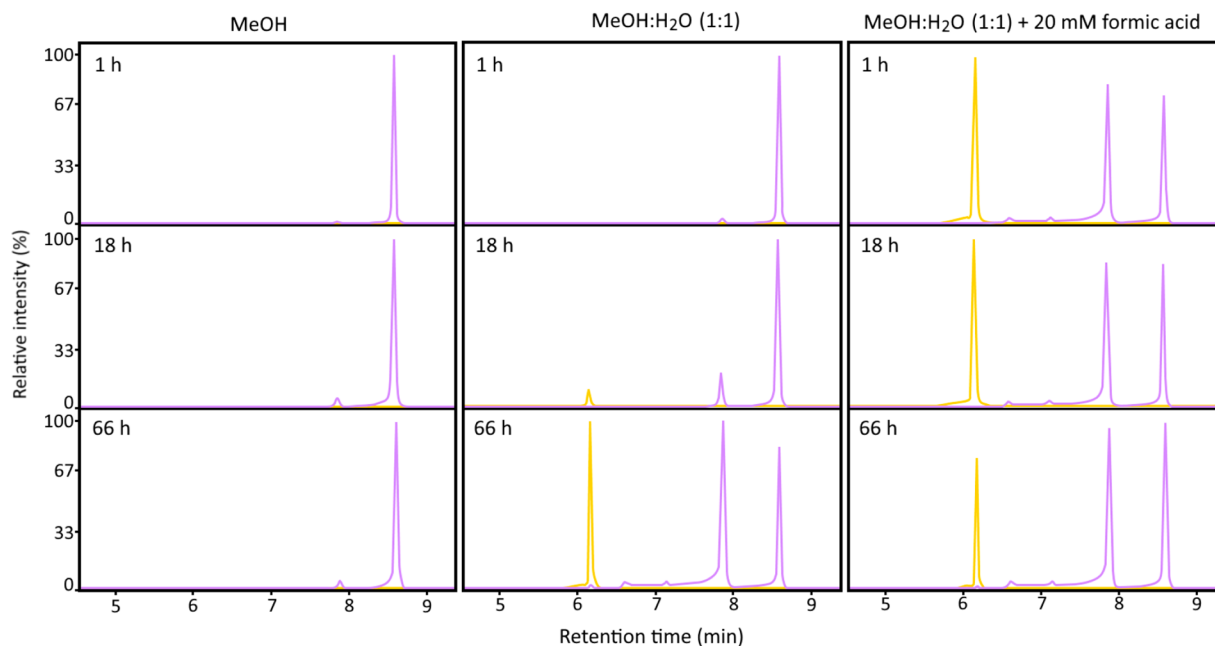


Figure 4. Stability studies on **1**. Studies carried out at 4–5 °C under neutral and acidic conditions were monitored by LC-MS (C18, H₂O/MeCN/20 mM formic acid, gradient elution, NH₄⁺ adducts). GDA and GDB (*m/z* 786) are presented in purple with retention times of 8.6 and 7.9 min, respectively. GDC (*m/z* 804) in yellow with retention time of 6.2 min.

GDB eluted at 27.0–28.7 and 20.8–21.9 min, respectively (HPLC, C18 column, isocratic elution with 80% MeOH/H₂O, diode array detection).¹³ An additional major component was observed, eluting at ~10 min with $\lambda_{\text{max}} \sim 220$ nm. Takeda did not pursue the structure of that compound, but, based on the relative retention time and the UV spectrum, a tentative assignment can be made as **7**.

In solution, GDC undergoes slow conversion to an isomeric substance. After storage in MeOH for 6 weeks at –20 °C, ~20% the new substance was present with no other new products being observed. Its UV spectrum was essentially identical to that of **7**. Formation of the substance was found to be irreversible.

Stability Studies on GDC (1). Stability studies were carried out on GDA as a preliminary step in elucidation of the relationships among the congeners. The studies assessed the stability of **1** under three solvent conditions: (1) anhydrous MeOH, (2) 1:1 MeOH/H₂O, and (3) 1:1 MeOH/H₂O containing 20 mM formic acid. The solutions were monitored by LC-MS after storage at 4–5 °C for 1, 18, and 66 h (Figure 4). The stability of **1** was excellent in anhydrous MeOH, showing only trace conversion to GDB within 66 h. Stability in 1:1 MeOH/H₂O was noticeably poorer with extensive conversion to GDB and GDC. Onofrio et al. have also observed instability of GDA in ultrapure H₂O (43% loss after 6 h) and even greater instability in filtered seawater (93% loss after 6 h).^{24–26} After 48 h, no GDA was detectable in filtered seawater. Under acidic conditions (20 mM formic acid), the conversion to GDB and GDC was greatly accelerated, reaching approximately the same state in only 1 h as after 66 h in 1:1 MeOH/H₂O.

The conversion process is reversible, approaching an equilibrium state in which the peak areas of the three congeners are comparable (Figure 5). On standing for longer periods or at higher temperatures, conversion to seco acids was also observed. An implication of this experiment is that

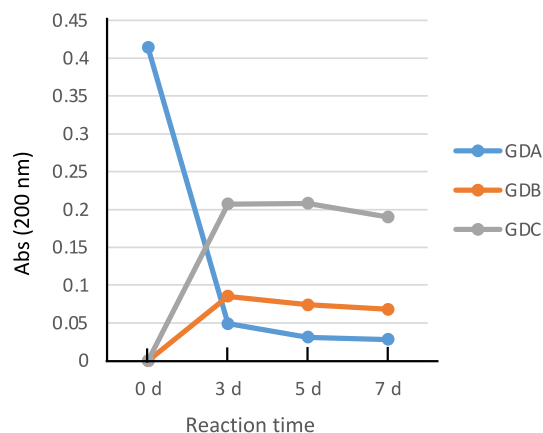


Figure 5. Equilibration of GDA, GDB, and GDC. GDA (100 μ g), was dissolved in 1:1 MeOH/H₂O (0.5 mL) and heated at 32 °C for 7 days. The reaction was periodically monitored by HPLC (Waters XB C18 column, 4.6 \times 150 mm), flow rate 1.0 mL/min, solvents (A) H₂O, (B) MeCN, gradient: 50% B to 99% B over 16 min.

solutions of analytical standards of GDA and some congeners of GDA can be expected to undergo degradation on storage in aqueous solutions or protic solvents, although the rate of degradation will be slower at low temperatures. We have not observed degradation of GDA in the solid state even on storage for several years at –20 °C. This observation would likely be true for the congeners, as well.

With 1:1 MeOH/H₂O and 0.1 mM hydrochloric acid, equilibration is expedited along with formation of minor additional products. TFA accelerated GDA–GDB–GDC equilibration even more. The minor products formed by HCl and TFA would be difficult to prepare in quantities sufficient for characterization. Equilibration with GDB and GDC was also observed in 1:1 aqueous acetonitrile (MeCN), but the process was slower than in aqueous MeOH. Equilibration in aqueous MeCN was accelerated by HCl, but again the process

was slower than observed for the HCl-catalyzed reaction in aqueous MeOH. The stability of GDA was excellent in dry, HPLC-grade MeCN.

The conversion of GDA to GDB could be either an S_N1 or S_N2 process. An acid-catalyzed S_N2 process would involve protonation of the C-15 oxygen atom followed by departure of the resulting hydroxy group simultaneous with bond formation by the 5-OH group. The 15-OH group would depart from the *re* face of C-11 (back face in Figure 6) as the 5-OH group

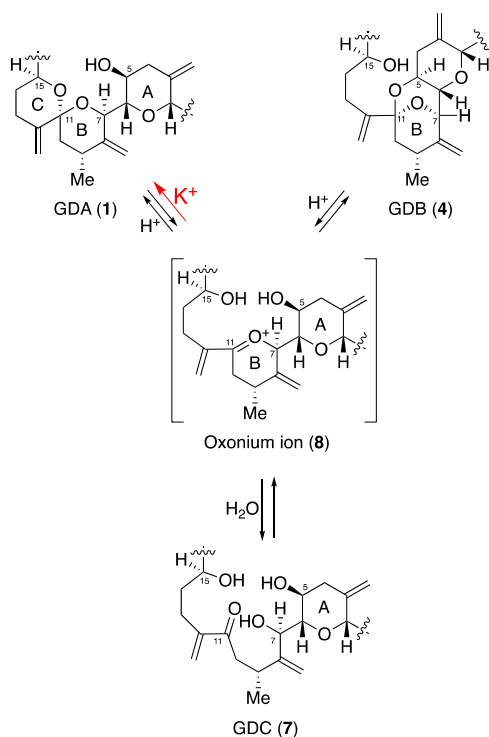


Figure 6. Interconversion of GDA, GDB, and GDC.

attacked on the *si* face (front face), leading to inversion of configuration at C-11. At the other extreme, an S_N1 process would involve departure of the 15-OH prior to entry of the 5-OH group with oxonium ion 8 being an intermediate in the process. In simple systems S_N1 or S_N2 processes can be distinguished by configurational analysis of the products since the S_N1 process would lack memory of the configuration of the starting material. In the present case both the departing and entering oxygen atoms are linked to C-11. As a consequence, the stereochemistry of product formation is structurally constrained, leading to inversion at C-11 irrespective of whether the process is S_N1 or S_N2 . Nevertheless, the process can be recognized as being S_N1 by the fact that intermolecular attack on the oxonium ion by H_2O competes with the intramolecular reaction. The attack by H_2O leads to formation of GDC (7).

Conversion of GDA to GDB is a reversible process, and the ratio of GDA and GDB is relatively immune to solvent effects because it depends on the free energies of the two compounds. The formation of GDC involves addition of a molecule of H_2O , so the ratios of GDC to GDA and GDB at equilibrium will depend not only on the free energies of the three substances but also on the concentration of H_2O in the reaction mixture. Generally, the equilibration studies using HPLC were carried out in 1:1 (v/v) MeOH/ H_2O because

MeOH was required to maintain homogeneity at the concentrations required for UV monitoring. Presumably, formation of GDC would be strongly favored under MeOH-free natural conditions. These processes are readily catalyzed by Brønsted acids that protonate electron-rich sites. The processes can also be catalyzed by Lewis acids. Catalysis of interconversion was observed with sodium ions. Formation of GDB and GDC from GDA occurred using 1% NaCl in 1:1 aqueous MeOH, although the equilibration was not as rapid as with proton acids.

Facile interconversion of GDA, GDB, and GDC occurs under very mild acidic conditions. The process is rapid in dilute HCl and formic acid but is observed even in aqueous MeOH. The interconversion presents a serious impediment to accurate quantification and to quantitative studies of toxicity. The interconversion of GDA, GDB, and GDC can be circumvented by use of alkaline conditions, but they present their own problems due to degradation of GDA, even under the mildly basic conditions of seawater.²⁴

Comparison of Chemical Properties of GDA, GDB, and GDC. The relative retention times of the three species on C18 chromatography columns are consistent with the assigned structures, with elution times in the order GDA > GDB > GDC with wide spacing between them when employing an aqueous MeCN gradient. The order of elution and differences in elution times can be rationalized by consideration of solvent access to hydroxy groups in the region of rings A, B, and C. GDA has a free hydroxy group at C-5, but the conformation as determined by NMR and X-ray crystallography places it close enough to O_B to form a hydrogen bond via a six-membered ring. The hydroxy group at C-15 is free in GDB. The conformation of GDB has not been established, but it is likely that the 15-hydroxy group hydrogen bonds to H_2O because intramolecular hydrogen bonding to O_A or O_B would involve larger rings. For GDC, the C-5, C-7, and C-15 hydroxy groups are all free. The GDC structure will be conformationally more mobile than those of GDA and GDB, so all hydroxy groups of GDC can be expected to have good access to H_2O . Likewise, the melting points of the three substances are consistent with the assigned structures: GDA 199.5–200 °C, GDB 120–121 °C, GDC ~100 °C dec. The structural changes associated with the thermal decomposition of GDC have not been studied.

The ultraviolet spectrum of GDB is similar to that of GDA, showing only end absorption at 200 nm, although the spectra differed slightly in the slope approaching 200 nm. End absorption is also observed with GDC, but the signature of GDC is a well-defined λ_{max} at 222 nm. The A_{200} value for GDC was approximately half those of GDA and GDB.

The electrospray mass spectra of GDA revealed preferences for formation of adducts with K^+ and NH_4^+ , while GDB and GDC showed preference for formation of adducts with Li^+ and Na^+ . None of the three goniodomins produced significant H^+ adducts, although fragmentation of the NH_4^+ adducts of GDA and GDB caused immediate loss of NH_3 to give protonated species that underwent further fragmentation. Numerous additional congeners have been observed in mass spectra of extracts of *Alexandrium* spp., but it is unlikely that sufficient amounts of them can ever be obtained to be able to carry out NMR studies. High-resolution collision-induced dissociation (CID) mass spectra of GDA, GDB, and GDC were recorded in anticipation that the fragmentation patterns might be of future value for assigning structures of other congeners. Tables in the Supporting Information list the measured exact masses of

major fragments along with calculated empirical formulas and proposed structural assignments of the fragment ions. The spectra of Na^+ and NH_4^+ adducts of GDA, GDB, and GDC were also acquired by LC-MS/MS runs with 2 mM ammonium formate in both eluents. It is apparent that GDA can undergo transformations not just to GDB and GDC but to other substances as well. Related structures can arise due to laboratory manipulations and spontaneously in the natural environment. Species with modified structures can also be formed by alterations in biosynthetic processes. An example of the latter was recently reported.^{16,18}

Differential Effects of Na^+ and K^+ on the Equilibration of Goniiodomin Congeners. We recently reported that TLC of GDA on silica gel plates that had been impregnated with alkali metal ions showed strong retardation of GDA by K^+ , Rb^+ , and Cs^+ but none by Li^+ or Na^+ .¹² The comparison of NaCl with KCl is shown in Figure 7. KCl (0.5%) caused strong retardation of GDA but NaCl (0.5%) caused virtually none.

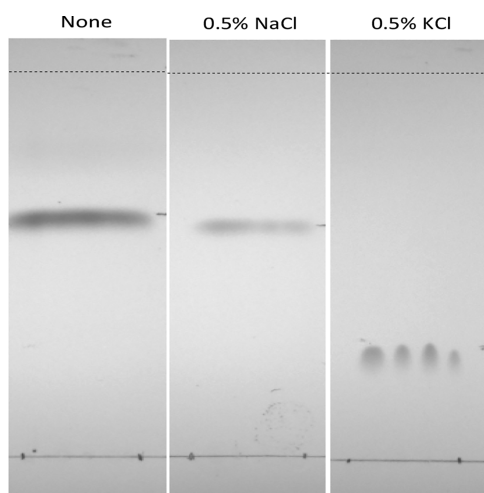


Figure 7. TLC of GDA on silica gel plates that have been modified with 0.5% NaCl or KCl in 1:1 (v/v) MeOH/H₂O; elution with 3:1 EtOAc/benzene; visualization with I₂ vapor. Adapted from ref 12.

The TLC phenomenon has been further investigated using HPLC to circumvent uncertainties concerning the amounts of alkali metal salts deposited on the TLC plates. HPLC is also a more sensitive technique for detecting formation of weak metal ion complexes. The HPLC study was carried out using C18 reversed-phase chromatography. Elution times for GDA were monitored with 3:1 (v/v) MeOH/H₂O isocratic eluents containing 0.0, 1.0, 10.0, and 100.0 mM solutions of NaCl and KCl. The ratios of retention times in the presence of KCl and NaCl are shown in Figure 8. K^+ strongly reduces the retention time of GDA; a similar but much weaker effect by NaCl is observed but only at the highest concentration of the salt, supporting the conclusion that Na^+ forms complexes but only weakly. Neither K^+ nor Na^+ caused significant retardation of either GDB or GDC.

In the solution conformation of GDA, rings A and E are turned outward, interfering with formation of metal ion complexes.¹³ NMR investigation of the effect of K^+ revealed that complexation brought about a major conformational change.¹² In the presence of K^+ the conformation of the macrocyclic ring is altered such that all five of the heterocyclic oxygen atoms are facing inward and can simultaneously complex with K^+ . Our attempts to prepare crystals of the K^+

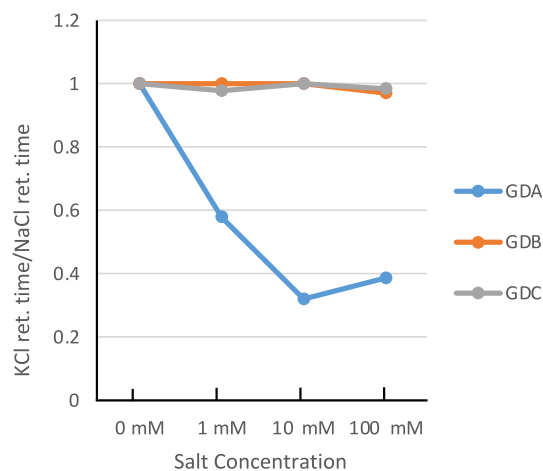


Figure 8. HPLC of GDA, GDB, and GDC. Ratios of retention times with varying concentrations of KCl and NaCl in eluent. Conditions: C18 reverse-phase HPLC employing isocratic elution with 3:1 (v/v) MeOH/H₂O, monitored by UV absorption at 205 nm.

complex suitable for X-ray crystallography have not been successful, but molecular dynamics (MD) yielded a model that provided insight into this cation effect (Figure 9).¹²

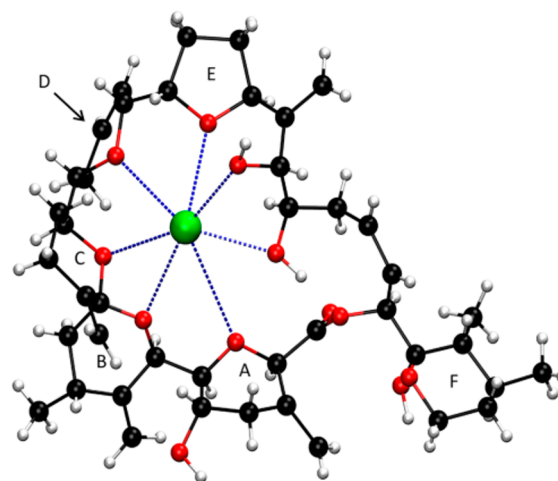


Figure 9. Model of the GDA: K^+ complex discovered by constrained MD simulation.

In light of this finding, the effects of Na^+ and K^+ on mixtures of the goniiodomin congeners were examined. In one experiment, equilibration of GDA with GDB and GDC was initiated using NaCl (100 mM) in 1:1 MeOH/H₂O (Table 2). After equilibrium was reached, KCl (100 mM) was added *without removal of the NaCl*. GDB and GDC underwent slow conversion back to GDA, demonstrating that stabilization of GDA by K^+ overwhelms the equilibration catalyzed by Na^+ .

The experiment was repeated using catalysis by 0.1 mM HCl. The acid accelerated both the conversion of GDA to GDB and GDC and their reversion to GDA (Figure 10). Panel A shows initiation of the experiment immediately prior to addition of the HCl to the GDA. Within 5 h, equilibration of GDA, GDB, and GDC was essentially complete (panel B). At that point, KCl was added to create a 100 mM solution. Monitoring of the reaction was continued, and reversion of GDB and GDC to GDA was observed. A chromatogram recorded at the 24 h point is shown in panel C. Disappearance

Table 2. Formation of Congeners of GDA in the Presence of Na⁺; Reversion to GDA upon Addition of K⁺

| time (h) | relative peak areas (%) | | | |
|----------|-------------------------|-------|-------|---------------------|
| | GDA | GDB | GDC | |
| 0 | 99.7 | 0.15 | 0.15 | NaCl added (100 mM) |
| 24 | 96.06 | 2.65 | 1.29 | |
| 96 | 86.69 | 7.59 | 5.72 | |
| 168 | 75.71 | 13.09 | 11.20 | |
| 264 | 56.87 | 18.53 | 24.61 | KCl added (100 mM) |
| 312 | 73.43 | 8.06 | 18.51 | |
| 480 | 82.67 | 4.19 | 13.14 | |
| 744 | 86.39 | 3.64 | 9.97 | |

of GDB occurred slightly faster than that of GDC. After 150 h, reconversion to GDA was essentially complete with only traces of GDB and GDC remaining (panel D).

Several things should be noted in these chromatograms. The intense signal at 1.4 min is produced by KCl. The shoulder at

1.7 min is due to goniiodomin-derived seco acids, the chemistry of which will be dealt with in a future publication. Addition of KCl provides partial protection against formation of the seco acid(s). Seco acid formation was also observed in the above NaCl/KCl experiment.

NMR Study of the Na⁺ Complex of GDA. Addition of sodium tetrakis[3,5-bis(trifluoromethyl)phenyl]borate (NaBARF₂₄, ~2 equiv) to GDA dissolved in benzene-*d*₆ yielded a suspension, from which particulate matter was removed by centrifugation. The supernatant was transferred to a 5 mm NMR tube. The ¹H NMR spectrum consisted of broad, poorly defined signals (spectrum not shown). Addition of 1% of MeOH-*d*₄ improved the resolution such that interpretable signals were present in the uncluttered 6.6–4.6 ppm region of the spectrum (panel A in Figure 11). Addition of a total of 5% of MeOH-*d*₄ gave further improvement (panel B). For comparison, panels C and D show the same region of the spectra of GDA and the K⁺ complex formed with KBARF₂₀.¹²

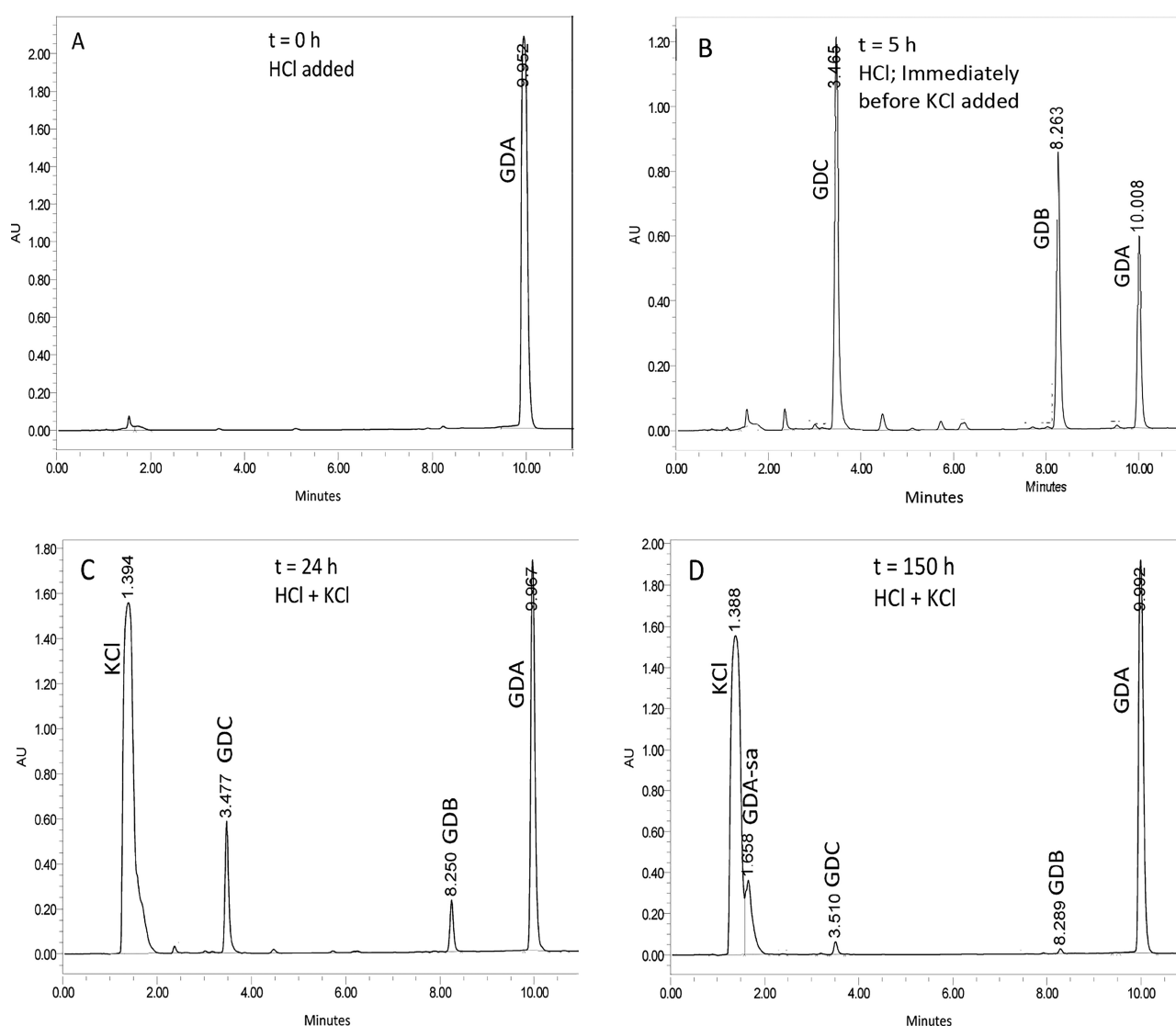


Figure 10. HPLC chromatograms of interconversion of goniiodomin congeners. 0.1 mM HCl-catalyzed conversion of GDA to a mixture with GDB and GDC, and 100 mM KCl-catalyzed reversion to GDA. (A) GDA in 1:1 (v/v) MeOH/H₂O immediately prior to addition of HCl. (B) Reaction mixture at equilibrium (5 h) immediately prior to addition of KCl (100 mM). (C) Reaction mixture after 24 h total. (D) Reaction mixture after 150 h total. HPLC conditions: C18 column, MeCN/H₂O gradient, UV detection 200 nm.

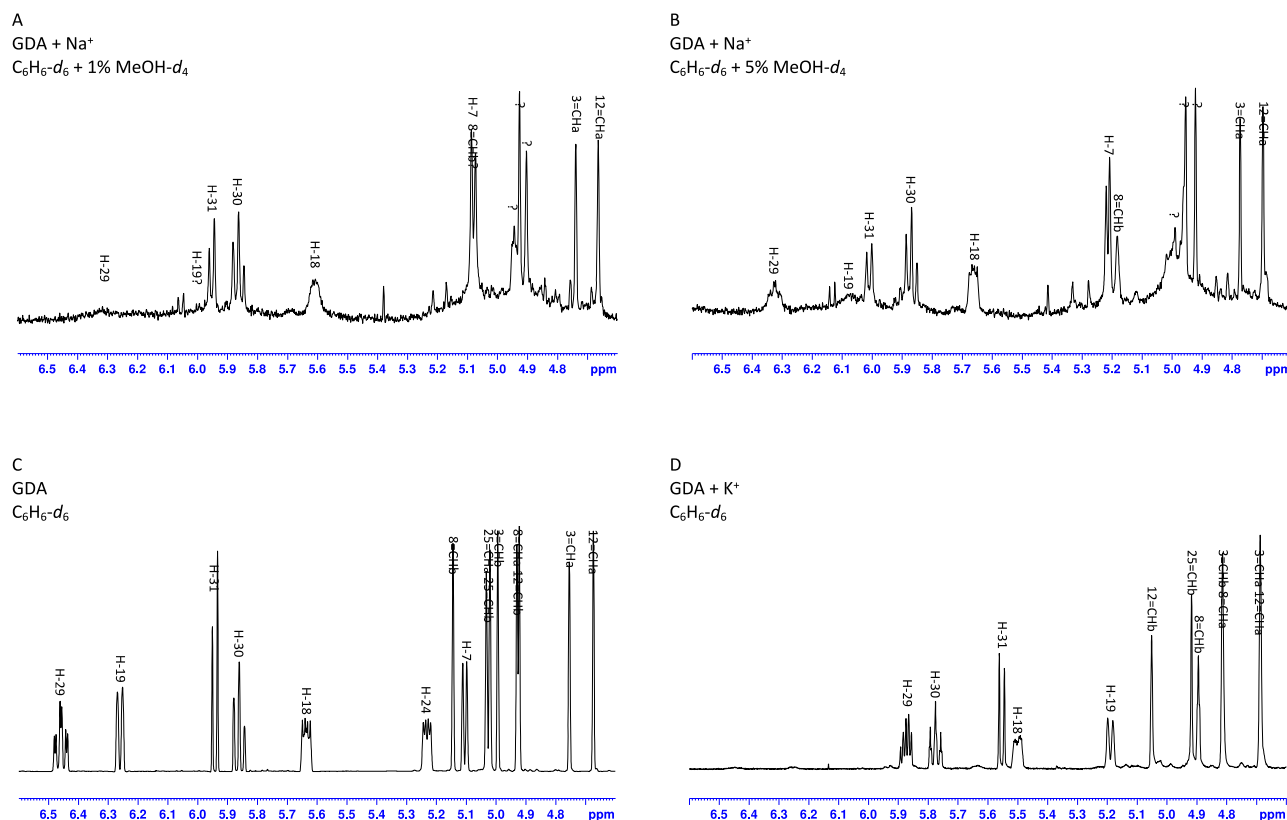


Figure 11. NMR spectra of GDA and GDA complexes with Na^+ and K^+ ions in benzene- d_6 . Region 4.6 and 6.6 ppm. (A) GDA + Na^+ + 1% MeOH- d_4 ; (B) GDA + Na^+ + 5% MeOH- d_4 ; (C) GDA; (D) GDA + K^+ . The spectra in panels A and B employed NaBARF_{24} ; panel D employed KBArF_{20} .

Table 3. ^1H NMR Assignments of Selected Signals for GDA, GDA- K^+ , and GDA- Na^+

| position | GDA ^a | GDA + $\text{K}^{+b,c}$ | GDA + Na^{+c} |
|----------|-----------------------------|-----------------------------------|------------------------|
| | δ , m (J in Hz) | δ , m (J in Hz) | δ , m (J in Hz) |
| 3=CHa | 4.76, s | 4.68, s | 4.96, s |
| H-7 | 5.09, d (8.4) | 4.51, brs | 5.21, d (6.6) |
| 8=CHb | 5.15, s | 4.90, s | 5.18, s |
| 12=CHa | 4.68, s | 4.68, s | 4.72, s |
| H-18 | 5.63, brdd | 5.50, brd (8.9) | 5.66, brm |
| H-19 | 6.23, brd (10.8) | 5.19, brd (5.19) | 6.08, brd (10.0) |
| H-29 | 6.42, ddd (12.0, 11.4, 3.6) | 5.88, ddd (10.7, 5.5, 5.5) | 6.33, brdd (6.3, 6.3) |
| H-30 | 5.84, dd (11.4, 10.2) | 5.79, dddd (10.6, 10.6, 2.0, 2.0) | 5.87, brdd (7.1, 7.1) |
| H-31 | 5.93, d (10.2) | 5.56, d (10.3) | 6.01, brd (10.2) |

^aReference 13; benzene- d_6 . ^bReference 12; benzene- d_6 . ^cPresent work; benzene- d_6 + 5% MeOH- d_4 .

Due to issues with commercial availability, different counterions were employed for the Na^+ and K^+ experiments.

The improved resolution of peaks in panel B permitted assignment of some of the ^1H signals (Table 3), in particular H-29, H-30, and H-31, by comparison of chemical shifts and multiplicities with those of GDA with confirmation by COSY cross-peaks of H-30 with H-29 and H-31. Identification could be made of 3=CHa, H-7, 8=CHb, 12=CHa, H-18, and H-19 on the basis of chemical shifts. We had previously observed that conversion of GDA to its K^+ complex caused strong shielding of numerous proton signals as exemplified by H-19, H-29, and H-31 (panel D), which had shifted to lower chemical shifts by 1.04, 0.54, and 0.37 ppm, respectively, so that no proton signals remained above 6 ppm.¹² For the Na^+ complex, this effect was not observed; the chemical shifts of all

three proton signals were still greater than 6 ppm. In fact, the spectrum of the Na^+ complex of GDA looked much more like that of GDA than that of the K^+ complex, leading to the conclusion that complexation with Na^+ is weak and fails to bring about the conformational shift that had been observed with K^+ . It is apparent from chromatographic data that the association of Na^+ with GDA is weaker than that of K^+ . Moreover, GDA elution is not retarded on NaCl-treated silica gel TLC plates.

Molecular Dynamics Simulations of Na^+ Binding to GDA. An investigation of the binding of Na^+ to GDA was carried out using molecular dynamics. Working with elevated concentrations of GDA to favor formation of oligomeric species, 2:1 complexes of GDA with Na^+ were observed. One example involved coordination of Na^+ with 26-OH and 27-OH

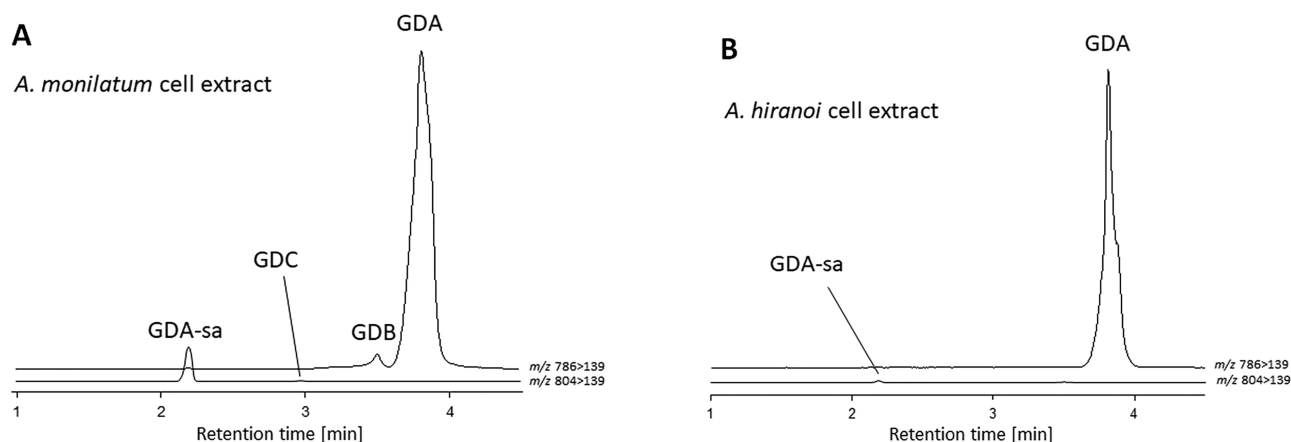


Figure 12. Extracted ion chromatograms (NH_4^+ adducts) of intracellular GDA, GDB, and GDC in *A. monilatum* (A) and *hiranoi* (B). Ion trace acquired using the m/z 786 > m/z 139 transition for GDA and GDB and m/z 804 > m/z 139 for GDC and GDA-sa.

of one of the GDA molecules (Na–O distances of 2.13 and 2.47 Å, respectively); coordination with a second GDA molecule involved its 5- and 26-OH groups (Na–O distances of 2.50 and 2.22 Å, respectively). All other oxygen atoms were too far from the Na^+ to contribute to stabilization of the complex. In contrast with the situation involving K^+ , MD simulations provided no evidence for the conformational change required to create a binding site for Na^+ comparable to that observed with K^+ .

Distribution of GDA, GDB, and GDC in *Alexandrium* Cells. An investigation was carried out on the intracellular distribution of GDA, GDB, and GDC in cultures of *A. monilatum* and *A. hiranoi*. Whereas *A. monilatum* cells were stored at -20°C for 2 months after harvest until extraction and analysis, *A. hiranoi* cells were extracted with MeOH immediately after harvest and the extract was stored at -20°C for 5 months until analysis. Both extracts were dominated by GDA, with the *A. monilatum* extract displaying small amounts of GDA-seco acid (GDA-sa), GDB, and traces of GDC (Figure 12A). In contrast, the *A. hiranoi* extract displayed only GDA plus traces of GDA-sa, no GDB or GDC (Figure 12B). The question of whether GDB and GDC are postharvest transformation products of GDA or true biosynthetic products in GD-producing species cannot be answered unambiguously with these data, but there is compelling evidence that GDA is readily transformed into GDB/C. It is reasonable to assume that these transformations also occur during storage, harvest, extraction, and even chromatographic analysis. Reanalysis of methanolic GD extracts revealed that the GD profiles were stable for up to nine months in this solvent (data not shown). In contrast, freezing of GD-containing cells and storage seems to induce transformation, probably through contact with H_2O resulting from disintegrated cells after a freeze/thaw cycle. This hypothesis would explain the difference seen in the GDB/C and GDA-sa content of the two samples.

CONCLUSIONS

Why is the behavior of Na^+ so different from that of K^+ ? In many respects the chemistry and physical properties of the two metal ions are very similar; however, the van der Waals radius of K is 2.75 Å, whereas that of Na is only 2.27 Å. K^+ can coordinate six or seven oxygen atoms, but Na^+ only five or six. Atomic radii of six- and seven-coordinated homoleptic K species are 1.38 and 1.46 Å, but five- and six-coordinated

homoleptic Na species are only 1.02 and 1.07 Å.²⁷ These facts plus the steric constraints placed on the GDA coordination sphere by the macrolide structure limit the number of coordination sites that can simultaneously be occupied to 1–2 less for Na^+ than for K^+ . An energetic problem is that formation of the metal complex requires displacement of coordinated H_2O or other solvent molecules and the enthalpy of hydration is significantly higher for Na^+ than K^+ (Na^+ 409 kJ/mol; K^+ 322 kJ/mol).²⁸ The net effect is that the energy of coordination of Na^+ with GDA is insufficient to compensate for the energetic costs of desolvation plus the conformational shift. As an alternative, sodium ions coordinate, but only weakly, at multiple sites on conformations of GDA similar to that of the uncomplexed compound, creating multidimensional oligomeric complexes.

Parallels exist between the K^+ selectivity of GDA and that of valinomycin, a depsipeptide ionophore that shows strong selectivity for K^+ over Na^+ . Valinomycin has two conformations, one with the amide carbonyl groups pointing outward to form hydrogen bonds with H_2O or other hydroxylic solvents and the other where they have been rotated inward so that the six carbonyl groups are octahedrally coordinated with K^+ in square bipyramidal geometry. The size of the valinomycin binding cavity is optimal for binding K^+ , but Na^+ is too small to make a snug fit. Rempe and co-workers have shown that conformational constraints physically prevent valinomycin from collapsing down around Na^+ .²⁹

GDA also has two families of stable conformations, identified here as A and B. The A family is represented by Takeda's solution conformation deduced from NMR spectra⁴ and our solid-state structure established by X-ray crystallography.¹² The B family is embodied in the GDA- K^+ complex. Interconversion between these two families of conformers is deemed to be rapid on the NMR time scale. The close similarity of the crystallographic structure of GDA to Takeda's NMR structure indicates that the A structures are more stable than the B to the extent that in the absence of K^+ no more than a small percentage of B is present in solutions of GDA. The free energy difference for the net reaction, $\text{GDA} + \text{K}^+ \rightarrow \text{GDA-K}^+$, must be sufficient to overcome not only the cost of the conformational shift but also that of desolvation of the K^+ . The same considerations exist for the sodium ion except that the heat of solvation is 87 kJ/mol higher. Complexation of K^+ with six or possibly seven oxygen atoms in GDA adequately

compensates for the energetic costs of desolvation and conformational shift, but Na^+ complexation with five oxygen atoms does not. Experimental evidence derived from chromatographic and spectroscopic studies reported herein indicate that Na^+ complexation occurs only with conformer A and even that occurs with low affinity. The consequences of this are that Na^+ causes GDA to convert to mixtures of GDA, GDB, and GDC, but K^+ , which binds selectively to GDA, converts GDB and GDC back to GDA *even when Na^+ is present*.

The present results may have consequences with respect to the biosynthesis of GDA. Drawing upon knowledge of the biosynthesis of other polyketides,³⁰ it seems likely that the acyl carrier protein thiol ester of GDA seco acid is the immediate precursor of GDA, but the conversion of GDC to GDA, which is observed in the presence of K^+ , raises the possibility that the final step carried out by the polyketide synthase might be formation of GDC prior to nonenzymatic formation of the spiro C–D ring system, the formation of which would be facilitated by the high intracellular concentration of K^+ .

Much progress has been made toward achieving a stereochemically defined total synthesis of GDA, but two troublesome steps remain: (1) formation of the spiro ring system constituting rings B and C and (2) closure of the macrocyclic ring.^{5–9,11,21–23} The observed K^+ -induced conversion of GDC to GDA could impact these efforts. Formation of a correctly configured spiro ring system is achieved more readily starting from GDC and probably from the seco acid of GDC than from the model systems that have been studied, because the stereochemical requirements imposed by the configurations at C-7- and C-15-hydroxy groups ensure the resulting spiro ring juncture has the correct configuration. In formation of the macrolide ring, complexation of the precursor seco acid with K^+ might pull the C-31 hydroxy group into close proximity to the carboxyl group, improving the probability of the correct cyclization occurring.

■ EXPERIMENTAL SECTION

General Experimental Procedures. GDA (1) was isolated from a bloom of *Alexandrium monilatum* that occurred in 2013 in the York River, VA, USA. Isolation of GDA was carried out by a published procedure adapted from the procedure of Sharma et al.^{1,2} Purity was assessed by ^1H NMR data and by TLC (Merck silica gel analytical plates 60 F254, 5 Å, 2.5 × 20 cm, 0.25 mm thickness), eluted with 3:1 (v/v) EtOAc/benzene; R_f ~0.60. GDA was visualized with iodine vapor or by spraying with ethanolic phosphomolybdic acid followed by development with heat. MeCN was HPLC grade. All other reagents were ACS grade or equivalent.

Stability Studies on GDA. Stability studies were undertaken with GDA in MeOH, MeOH/ H_2O (1:1), and MeOH/ H_2O (1:1) with 20 mM formic acid. Reactions were carried out at 4–5 °C and sampled after 1, 18, and 66 h. Analysis by HPLC–HRMS was undertaken on a Dionex Ultimate 3000 HPLC (Thermo Fisher Scientific) equipped with a Phenomenex Kinetex column (2.6 μm , C18, 100 Å, 100 mm × 2.1 mm) and coupled to a Bruker Maxis quadrupole time-of-flight (Q-TOF) MS. The column compartment was maintained at 40 °C, and a constant flow rate of 400 $\mu\text{L}/\text{min}$ was used. Chromatographic separation was achieved using gradient elution with eluent A (H_2O , 20 mM formic acid) and eluent B (MeCN, 20 mM formic acid). The gradient started at 10% B and finished at 100% B, over 10 min. All analyses were carried out with an electrospray ionization source with positive polarity and a scan range of m/z 300–2500 at a data acquisition rate of 2 spectra/s. The nebulizer gas was set to 1.8 bar, and the capillary voltage was 4500 V. The dry gas was set at 200 °C at a flow rate of 10 L/min. Samples were injected using 10 μL volumes. Full-scan spectra were recorded, and extracted ion chromatograms were used to display the acquired data. The ions used to represent

relative abundances of the different target ions were the ammonium adducts, m/z for GDA and GDB at 786 and for GDC at m/z 804. To correct for saturation effects in some samples, the second isotopomer of the ammonium adduct was utilized for relative compositions. The second isotopomer was utilized for all target ions, to maintain correct relative abundances. No corrections were made for ionization efficiencies.

Reactions of GDA and Congeners. Transformations of goniodomins to congeners were investigated by HPLC. New products were further characterized by MS and NMR. HPLC was carried out on a Waters Alliance e2695 separations module equipped with a model 2998 photodiode array detector (PDA) with both being operated with Waters Empower software. Reactions were carried out at ambient temperature unless otherwise noted using 12 × 32 mm screw cap sample vials (Waters) with the caps containing PTFE/silicone septa to permit direct evaluation by HPLC. Small-scale reactions were carried out on a scale of 0.2–0.5 mg generally using 1:1 MeOH/ H_2O solvent mixtures to provide for solubility of both the GDA and catalysts and analyzed periodically by HPLC on columns: Waters Bridge C18 3.5 μm , 4.6 × 150 mm and Waters Spherosorb ODS2 5 μm , 4.6 × 150 mm. Elution employed MeOH/ H_2O or MeCN/ H_2O isocratically or in gradients. Effluent was monitored at 200 nm plus a longer wavelength with 254 nm being chosen for scouting runs and 222 nm for specific monitoring of GDC. Molar absorptivity of GDC at 200 nm is about half those of GDA and GDB. The PDA software permitted full UV spectra to be recorded on peaks of interest. Samples for MS analysis were collected and evaporated to dryness with a Savant SpeedVac. Those that contained salts were evaporated and then triturated with CHCl_3 or C_6H_6 . The solvent was removed by SpeedVac. Those that contained acids were taken up in C_6H_6 or CHCl_3 , which was washed with H_2O , and then the organic solution was dried (Na_2SO_4) and evaporated to dryness. All samples were taken up in MeOH for MS analysis.

Reactions were scaled up to 2.5–5 mg when larger quantities of GDB and GDC were required for NMR spectroscopy and other purposes. For example, GDA (2.8 mg) was treated with a mixture of MeCN (1.00 mL), H_2O (0.4 mL), and 1 mM aqueous HCl (0.15 mL) at ambient temperature. Progress of the reaction was monitored by HPLC using Phenomenex C18 Luna (250 mm × 4.6 mm, 5 μm) columns with gradient elution at 1 mL/min (solvent A: H_2O , solvent B: MeCN, flow rate: 1 mL/min; gradient: 65% B to 90% B over 15 min, 90% B to 99% B over 5 min, hold at 99% for 2 min, return to 65% B over 2 min, detection at 200 and 254 nm). Retention times: GDA, 15.19 min, GDB, 10.93 min, GDC, 4.55 min. The reaction reached equilibrium within 4 d, at which point it was terminated by evaporation using a Büchi Rotavap and further dried with a lyophilizer. Isolation of GDA, -B, and -C was carried out by HPLC using a semipreparative Phenomenex C18 Luna (250 mm × 10 mm, 5 μm) column with gradient elution at 2.5 mL/min (solvent A: H_2O , solvent B: MeCN, flow rate: 2.5 mL/min; gradient: 65% B to 90% B over 10 min, hold at 90% B 10 min, return to 65% B over 3 min, detection at 210 nm). Retention times: GDA, 14.38 min, GDB, 11.53 min, GDC, 6.13 min. The three fractions were collected manually, concentrated to remove the MeCN using a Büchi Rotavap, and fully dried with a lyophilizer. The resulting materials were stored solvent-free at –20 °C to avoid degradation because interconversion and other degradation had been observed in hydroxylic solvents and also in non-hydroxylic solvents if they picked up moisture from the air. Similar preparative procedures were used when samples of the three goniodomins that had been prepared with phosphate and other buffers were being collected by HPLC except, after evaporation of the solvent, the residues were partitioned between water and either C_6H_6 or CHCl_3 or directly extracted with one of these solvents.

Goniodomin C (7) Mass Spectrometry. High-resolution mass spectra were acquired on a Bruker 10 T APEX-Qe FT-ICR mass spectrometer at Old Dominion University, Norfolk, VA, using electrospray ionization. The samples were introduced by direct infusion of a MeOH solution. CID spectra were acquired using an 8 Da isolation window with optimized CI voltage. Empirical formulas were assigned using ChemCalc.³¹

Two algal species were used for mass spectrometric GD analyses. *Alexandrium monilatum* strain YRK2007 was isolated from York River (Virginia, USA) in 2007 and was identified by light microscopy and LSU gene sequencing (unpublished). *Alexandrium hiranoi* strain CCMP2215 originally isolated from Japan was obtained from the National Center for Marine Algae and Microbiota (NCMA) at Bigelow.³² Both strains were grown at 20 °C with a photon flux density of 80 $\mu\text{E m}^{-2} \text{s}^{-1}$ (16:8 h light/dark photocycle) in K-medium³³ prepared with sterile-filtered (0.2 μm VacuCap filters, Pall Life Sciences) North Sea seawater adjusted to a salinity of 20 (pH adjusted to 8.0). A 50 mL amount of each species was harvested by centrifugation (Eppendorf 5810R, Eppendorf; 1000g, 10 min). Each pellet was transferred to a microtube, again centrifuged (Eppendorf 5415; 1000g, 5 min), and stored at -20 °C.

For the extraction of goniodomins, 400 μL of MeOH was added to the cell pellets. To each sample was added 0.9 g of Lysing Matrix D (Thermo Savant) as well. After sealing and vortexing the cryovials, cells were lysed by reciprocal shaking at maximum speed (6.5) for 45 s in a Bio 101 FastPrep device (Thermo Savant). Subsequently, homogenates were centrifuged at 16100g and 10 °C for 5 min (5415R, Eppendorf). The extracts were transferred to centrifugation filters with a pore size of 0.45 μm (Millipore Ultrafree) and centrifuged at 16100g and 10 °C for 1 min. The filtrates were finally transferred to HPLC sample vials (2 mL, Agilent), and vials were sealed with crimp caps (Agilent). Samples were stored at -20 °C until measurement.

Ultraperformance liquid chromatography (UPLC) coupled with tandem quadrupole mass spectrometry (LC-MS/MS) was used for the determination of GDs. The UPLC system included a column oven, an autosampler, and a binary pump (AQUITY I UPLC Class, Waters). The separation was carried out on an RP-18 column (Purospher STAR end-capped (2 μm) Hibar HR 50-2.1 UPLC, Merck) equipped with a precolumn (0.5 μm , OPTSSOLV EXP, Sigma-Aldrich). This system was coupled to a triple quadrupole mass spectrometer (Xevo TQ-XS, Waters). Data were acquired and analyzed with Masslynx (version 4.2, Waters). In addition to the mass transitions defined in the Selected Reaction Monitoring (SRM) mode, goniodomins were identified by the retention times of the respective pure compounds. Flow rate was 0.6 mL/min, and eluent A consisted of aqueous 6.7 mM ammonia and eluent B of 6.7 mM ammonia in MeCN/H₂O (9:1 v/v). A linear gradient was performed from 10% B to 90% B within 1.5 min. The mass transitions used for NH₄⁺ adducts were m/z 786 > m/z 139 for GDA and GDB and m/z 804 > m/z 139 for GDC and an unidentified isomer of GDC. A standard solution of 500 pg/ μL GDA was used for external calibration.

NMR Studies of GDB and GDC and of the Na⁺ Complex of GDA. NMR spectra (Table 1) were acquired using a 14.0 T Bruker magnet equipped with a Bruker AV-III console operating at 600.13 MHz. All spectra were acquired at 300 K in 5 mm NMR tubes using a Bruker 5 mm TCI cryogenically cooled NMR probe optimized for ¹H detection. Chemical shifts were referenced internally to benzene-*d*₆ (7.15 ppm), which also served as the ²H lock solvent.

The NMR sample of the Na⁺ complex of GDA was prepared by adding ~3 mg of NaBArF₂₄ to ~2 mg of GDA in ~0.6 mL of benzene-*d*₆ in a 5 mm NMR tube, leading to a suspension, which was centrifuged, and the supernatant was transferred to a fresh 5 mm NMR tube. The ¹H spectrum of the supernatant (not shown) contained only broad, undecipherable signals. Addition of (1%) MeOH-*d*₄ gave a ¹H spectrum with improved resolution, and 5% MeOH-*d*₄ gave sufficient resolution that selected protons could be assigned (panels A and B in Figure 11 and Table 3).

¹H NMR spectral parameters included 32K data points, a 13 ppm sweep width, a recycle delay of 1.5 s, and 32 scans. The data were processed using Gaussian modification (LB -1, GB 0.1) to enhance the peak shapes of multiplets. For 2D ¹H-¹H COSY, experimental conditions included a 2048 × 512 data matrix, a 13 ppm sweep width, a recycle delay of 1.5 s, and 4 scans per increment. The data were processed using a squared sinebell window function, symmetrized, and displayed in magnitude mode. Multiplicity-edited HSQC spectra

were acquired using a 1024 × 256 data matrix, a ¹J_{C-H} value of 145 Hz, which resulted in a multiplicity selection delay of 34 ms, a recycle delay of 1.5 s, and 32 scans per increment along with GARP decoupling on ¹³C during the acquisition time (150 ms). The data were processed using a $\pi/2$ shifted squared sine window function and displayed with CH/CH₃ signals phased positive and CH₂ signals phased negative. ¹J_{C-H} filtered HMBC experiments were acquired using a 2048 × 256 data matrix, a ¹J_{C-H} value of 9 Hz for detection of long-range couplings, resulting in an evolution delay of 55 ms, a ¹J_{C-H} filter delay of 145 Hz (34 ms) for the suppression of one-bond couplings, a recycle delay of 1.5 s, and 128 scans per increment. The HMBC data were processed using a $\pi/2$ shifted squared sine window function and displayed in magnitude mode.

Molecular Dynamics Studies of the Na⁺ Adduct of GDA. Molecular dynamics simulations were performed using version 5.0-rc1 of the GROMACS simulation package.^{33–36} The equations of motion were integrated using the leapfrog algorithm with a time step of 1 fs, and the temperature was maintained using a Nosé–Hoover thermostat with a coupling time of 2 ps.^{37,38} The real space portions of the van der Waals and Coulombic potentials were cut off at 1.2 nm, and the reciprocal-space part was evaluated using the particle-mesh Ewald method.³⁹ The mesh width was set to 0.1 nm, and a fourth-degree polynomial was used. The GROMOS 53a6 force field was used to model all of the bonded and nonbonded interactions.⁴⁰

Lennard-Jones parameters were used for the Na⁺, and geometric combination rules were utilized. No counterion was added. Instead, the simulations were run with a negative uniform background charge to compensate for the positive charge of Na⁺. Two GDA molecules, constituting the coordinates from the structure obtained by X-ray diffraction, were placed in a cubic simulation box utilizing periodic boundary conditions and an edge length 7.5 nm. The GDA molecules were solvated by 2758 benzene molecules, and the system was annealed from 0 to 300 K over 7.5 ns; this final temperature was then maintained for another 2.5 ns to obtain an equilibrated conformation. The equilibrated structure was then altered 20 times by randomly replacing one benzene molecule with one Na⁺. These 20 structures were subsequently run for 20 ns.

■ ASSOCIATED CONTENT

Supporting Information

The Supporting Information is available free of charge at <https://pubs.acs.org/doi/10.1021/acs.jnatprod.1c00586>.

NMR spectra of GDC with peak assignments; lists of CID fragment ions for GDA, GDB, and GDC with assigned empirical formulas and proposed structures (PDF)

■ AUTHOR INFORMATION

Corresponding Author

Thomas M. Harris – Department of Chemistry, Vanderbilt University, Nashville, Tennessee 37235, United States; Virginia Institute of Marine Science (VIMS), Gloucester Point, Virginia 23062, United States; orcid.org/0000-0002-3062-344X; Phone: +1-804-776-6987; Email: thomas.m.harris@vanderbilt.edu

Authors

Constance M. Harris – Department of Chemistry, Vanderbilt University, Nashville, Tennessee 37235, United States

Bernd Krock – Alfred Wegener Institut-Helmholtz Zentrum für Polar- und Meeresforschung (AWI), 27570 Bremerhaven, Germany

Urban Tillmann – Alfred Wegener Institut-Helmholtz Zentrum für Polar- und Meeresforschung (AWI), 27570 Bremerhaven, Germany

Craig J. Tainter – Department of Chemistry, Vanderbilt University, Nashville, Tennessee 37235, United States

Donald F. Stec – Department of Chemistry, Vanderbilt University, Nashville, Tennessee 37235, United States

Aaron J. C. Andersen – Department of Biotechnology and Biomedicine, Søtofts Plads, Technical University of Denmark, 2800 Kgs., Lyngby, Denmark

Thomas O. Larsen – Department of Biotechnology and Biomedicine, Søtofts Plads, Technical University of Denmark, 2800 Kgs., Lyngby, Denmark

Kimberly S. Reece – Virginia Institute of Marine Science (VIMS), Gloucester Point, Virginia 23062, United States

Complete contact information is available at:

<https://pubs.acs.org/10.1021/acs.jnatprod.1c00586>

Notes

The authors declare no competing financial interest.

ACKNOWLEDGMENTS

Support for this work was provided by NOAA (ECOHAB grant #NA17NOS4780182), by the Helmholtz-Gemeinschaft Deutscher Forschungszentren through the research program “Changing Earth – Sustaining our Future” of the Alfred-Wegener-Institut Helmholtz-Zentrum für Polar- und Meeresforschung, and by Vanderbilt University and the Virginia Institute of Marine Science. We acknowledge NIH grant S10 RR019022, which funded the purchase of the Bruker AV600 NMR spectrometer and accessories. We are grateful to R. E. O’Brien (William & Mary) for assistance with ultraviolet spectra and I. Ruhl (Old Dominion Univ.) for high-resolution mass spectra. Contribution #4040 of the Virginia Institute of Marine Science, William & Mary, and publication ECO995 of the NOAA NCCOS grant program.

REFERENCES

- (1) Sharma, G. M.; Michaels, L.; Burkholder, P. R. *J. Antibiot.* **1968**, *21*, 659–664.
- (2) Harris, C. M.; Reece, K. S.; Stec, D. F.; Scott, G. P.; Jones, W. M.; Hobbs, P. L. M.; Harris, T. M. *Harmful Algae* **2020**, *91*, 101707.
- (3) Murakami, M.; Makabe, K.; Yamaguchi, K.; Konosu, S. *Tetrahedron Lett.* **1988**, *29*, 1149–1152.
- (4) Takeda, Y.; Shi, J.; Oikawa, M.; Sasaki, M. *Org. Lett.* **2008**, *10*, 1013–1016.
- (5) Kawashima, Y. *Studies toward the total synthesis of amphidionolide N and goniodomin A*. Ph.D. Dissertation, Tohoku University, Sendai, Japan. Abstract. <http://hdl.handle.net/10097/00122676a>, 2017.
- (6) Fujiwara, K.; Naka, J.; Katagiri, T.; Sato, D.; Kawai, H.; Suzuki, T. *Bull. Chem. Soc. Jpn.* **2007**, *80*, 1173–1186.
- (7) Saito, T.; Fuwa, H.; Sasaki, M. *Org. Lett.* **2009**, *11*, 5274–5277.
- (8) Fuwa, H.; Nakajima, M.; Shi, J.; Takeda, Y.; Saito, T.; Sasaki, M. *Org. Lett.* **2011**, *13*, 1106–1109.
- (9) Saito, T.; Fuwa, H.; Sasaki, M. *Tetrahedron* **2011**, *67*, 429–445.
- (10) Nakajima, M. *Synthetic study of goniodomin A*. Ph.D. dissertation (abstract), Tohoku Univ., Sendai, Japan. <http://hdl.handle.net/10097/58723>, 2014.
- (11) Fuwa, H.; Matsukida, S.; Miyoshi, T.; Kawashima, Y.; Saito, T.; Sasaki, M. *J. Org. Chem.* **2016**, *81*, 2213–2227.
- (12) Tainter, C. J.; Schley, N. D.; Harris, C. M.; Stec, D. F.; Song, A. K.; Balinski, A.; May, J. C.; McLean, J. A.; Reece, K. S.; Harris, T. M. *J. Nat. Prod.* **2020**, *83*, 1069–1081.
- (13) Takeda, Y. *Stereochemical assignment of goniodomin A, an actin-targeting polyether macrolide*. Ph.D. dissertation, Tohoku Univ., Sendai, Japan. <http://hdl.handle.net/10097/34613c>, 2008. The depiction of the conformation of GDA in the dissertation is that of *ent*-GDA, but the experimental data in the dissertation and the resulting

publication⁴ establish the absolute configuration of GDA as depicted herein in Figure 1.

(14) Sasaki, K.; Wright, J. L. C.; Yasumoto, T. *J. Org. Chem.* **1998**, *63*, 2475–2480.

(15) Espiña, B.; Cagide, E.; Louzao, M. C.; Vilariño, N.; Vieytes, M. R.; Takeda, Y.; Sasaki, M.; Botana, L. M. *Toxicol. Lett.* **2016**, *250–251*, 10–20.

(16) Krock, B.; Tillmann, U.; Wen, Y.; Hansen, P. J.; Larsen, T. O.; Andersen, A. J. C. *Toxicon* **2018**, *155*, 51–60.

(17) Kremp, A.; Hansen, P. J.; Tillmann, U.; Savela, H.; Suikkanen, S.; Voss, D.; Barrera, F.; Jacobsen, H. H.; Krock, B. *Harmful Algae* **2019**, *87*, 101622.

(18) Harris, C. M.; Reece, K. S.; Harris, T. M. *Toxicon* **2020**, *188*, 122–126.

(19) Satake, M.; Ofuji, K.; Naoki, H.; James, K. J.; Furey, A.; McMahon, T.; Silke, J.; Yasumoto, T. *J. Am. Chem. Soc.* **1998**, *120*, 9967–9968.

(20) Nicolaou, K. C.; Murphy, F.; Barluenga, S.; Ohshima, T.; Wei, H.; Xu, J.; Gray, D. L. F.; Baudoin, O. *J. Am. Chem. Soc.* **2000**, *122*, 3830–3838.

(21) Nakajima, M.; Fuwa, H.; Sasaki, M. *Bull. Chem. Soc. Jpn.* **2012**, *85*, 948–956.

(22) Katagiri, T.; Fujiwara, K.; Kawai, H.; Suzuki, T. *Tetrahedron Lett.* **2008**, *49*, 233–237.

(23) Katagiri, T.; Fujiwara, K.; Kawai, H.; Suzuki, T. *Tetrahedron Lett.* **2008**, *49*, 3242–3247.

(24) Onofrio, M. D. *Spatial and Temporal Distribution of Phycotoxins in Chesapeake Bay: Method Development and Application*. M.S. Thesis, William & Mary, Virginia Institute of Marine Science: [10.25773/v5-z6gg-jz22](https://doi.org/10.25773/v5-z6gg-jz22), pp 118 and 155–156, 2020.

(25) Onofrio, M. D.; Mallet, C. R.; Place, A. R.; Smith, J. L. *Toxins* **2020**, *12*, 322.

(26) Onofrio, M. D.; Egerton, T. A.; Reece, K. S.; Pease, S. K.D.; Sanderson, M. P.; Jones, W., III; Yeagan, E.; Roach, A.; DeMent, C.; Wood, A.; Reay, W. G.; Place, A. R.; Smith, J. L. *Harmful Algae* **2021**, *103*, 101993.

(27) Mähler, J.; Persson, I. *Inorg. Chem.* **2012**, *51*, 425–438.

(28) Smith, D. W. *J. Chem. Educ.* **1967**, *54*, 540–542.

(29) Varma, S.; Sabo, D.; Rempe, S. B. *J. Mol. Biol.* **2008**, *376*, 13–22.

(30) Wan, X.; Yao, G.; Liu, Y.; Chen, J.; Jiang, H. *Mar. Drugs* **2019**, *17*, 594.

(31) Patiny, L.; Borel, A. *J. Chem. Inf. Model.* **2013**, *53*, 1223–1228.

(32) Keller, M. D.; Selvin, R. C.; Claus, W.; Guillard, R. R. L. J. *Phycol.* **1987**, *23*, 633–638.

(33) Berendsen, H. J. C.; van der Spoel, D.; van Drunen, R. *Comput. Phys. Commun.* **1995**, *91*, 43–56.

(34) Hess, B.; Kutzner, C.; van der Spoel, D.; Lindahl, E. *J. Chem. Theory Comput.* **2008**, *4*, 435–447.

(35) Lindahl, E.; Hess, B.; van der Spoel, D. *J. Mol. Model.* **2001**, *7*, 306–317.

(36) van der Spoel, D.; Lindahl, E.; Hess, B.; Groenhof, G.; Mark, A. E.; Berendsen, H. J. C. *J. Comput. Chem.* **2005**, *26*, 1701–1718.

(37) Hoover, W. G. *Phys. Rev. A: At, Mol, Opt. Phys.* **1985**, *31*, 1695–1697.

(38) Nosé, S. *J. Chem. Phys.* **1984**, *81*, 511–519.

(39) Essmann, U.; Perera, L.; Berkowitz, M. L.; Darden, T.; Lee, H.; Pedersen, L. G. *J. Chem. Phys.* **1995**, *103*, 8577–8593.

(40) Oostenbrink, C.; Villa, A.; Mark, A. E.; van Gunsteren, W. F. *J. Comput. Chem.* **2004**, *25*, 1656–1676.